Toward effective and reliable fluorescence energies in solution by a new state specific polarizable continuum model time dependent density functional theory approach

Roberto ImprotaGiovanni Scalmani and Michael J. FrischVincenzo Barone

Citation: The Journal of Chemical Physics **127**, 074504 (2007); doi: 10.1063/1.2757168
View online: http://dx.doi.org/10.1063/1.2757168
View Table of Contents: http://aip.scitation.org/toc/jcp/127/7
Published by the American Institute of Physics

Toward effective and reliable fluorescence energies in solution by a new state specific polarizable continuum model time dependent density functional theory approach

Roberto Improta[a)]
Dipartimento di Chimica, Università Federico II, Complesso Monte S. Angelo, via Cintia, I-80126 Napoli, Italy and Istituto di Biostrutture e Bioimmagini-CNR, via Mezzocannone 16, 80134 Napoli, Italy

Giovanni Scalmani and Michael J. Frisch
Gaussian, Inc., Wallingford, Connecticut 06492, USA

Vincenzo Barone
Dipartimento di Chimica, Università Federico II, Complesso Monte S. Angelo, via Cintia, I-80126 Napoli, Italy

(Received 18 April 2007; accepted 19 June 2007; published online 17 August 2007)

A state specific (SS) model for the inclusion of solvent effects in time dependent density functional theory (TD-DFT) computations of emission energies has been developed and coded in the framework of the so called polarizable continuum model (PCM). The new model allows for a rigorous and effective treatment of dynamical solvent effects in the computation of fluorescence and phosphorescence spectra in solution, and it can be used for studying different relaxation time regimes. SS and conventional linear response (LR) models have been compared by computing the emission energies for different benchmark systems (formaldehyde in water and three coumarin derivatives in ethanol). Special attention is given to the influence of dynamical solvation effects on LR geometry optimizations in solution. The results on formaldehyde point out the complementarity of LR and SS approaches and the advantages of the latter model especially for polar solvents and/or weak transitions. The computed emission energies for coumarin derivatives are very close to their experimental counterparts, pointing out the importance of a proper treatment of nonequilibrium solvent effects on both the excited and the ground state energies. The availability of SS-PCM/TD-DFT models for the study of absorption and emission processes allows for a consistent treatment of a number of different spectroscopic properties in solution. © *2007 American Institute of Physics*. [DOI: 10.1063/1.2757168]

I. INTRODUCTION

Fluorescence and phosphorescence spectroscopies have always been among the most powerful techniques for studying the structure and the properties of excited states.[1,2] In more recent years, due to the rapid advances in the development of time-resolved ultrafast spectroscopy, fluorescence upconversion experiments have provided fundamental insights on the excited state dynamics of several interesting systems, ranging from small/medium size organic molecules to complex macromolecular systems of biological or technological interest.[3] The interpretation of such sophisticated experiments was benefited by the contemporary advances in the development of effective and reliable computational methods for the study of excited electronic states, allowing for the accurate description of the structure and the properties of compounds of increasing size.[4,5] In this respect, the results obtained by the accurate, but computational expensive, post-self-consistent-field methods have been integrated by an increasing number of studies employing methods rooted in the time dependent density functional theory (TD-DFT).[4,5] As a consequence, several quantum mechanical methods (each one with its advantages and its drawbacks) are nowadays available to compute the excited state structure/properties of sizeable molecules, at least in the gas phase, as witnessed by the excellent agreement between the experimental and computational absorption spectra obtained for several systems.[6–10]

However, the computation of absorption and emission spectra in solution involves additional problems, as suggested by the smaller number of studies in the field.[11,12] Electron excitation/emission is indeed an intrinsically dynamic process, and thus it is important that the characteristic times of solvent degrees of freedom are taken into the proper account. This problem can be treated by means of molecular simulation techniques, explicitly considering solvent molecules.[13] Alternatively, the so called continuum models have become powerful tools for the quantum mechanical study of both ground and excited states.[11,14–19] Different strategies have been devised to study time dependent phenomena,[11,16–19] such as the formation and the relaxation of excited electronic states, within the framework of continuum models (see Ref. 20 for more details). In the following we will make specific reference to the so called polariz-

[a)]Electronic mail: robimp@unina.it

able continuum model (PCM), which is, in our opinion, particularly suitable from the point of view of both physical soundness and computational effectiveness.[11]

Time dependent solvation effects can be described in the PCM framework by introducing a time dependence in the apparent surface charges.[20,21] A simpler, but effective and often used, approach relies instead on the definition of two extreme time regimes:[22,23] (i) the nonequilibrium regime, in which only solvent electronic polarization (fast degree of freedom) is in equilibrium with the excited state electron density of the solute, while the slow solvent degrees of freedom remain equilibrated with the ground state electron density; (ii) the fully equilibrated regime, where all the solvent degrees of freedom are in equilibrium with the electron density of the state of interest. In the framework of continuum solvation models the two situations are ruled by two different dielectric constants. In the nonequilibrium case, the reaction field due to the fast solvent degrees of freedom depends on the dielectric constant at optical frequency (ϵ_{opt}, usually related to the square of the solvent refractive index n, $\epsilon_{opt}=n^2$). Equilibrium solvation is instead ruled by the static dielectric constant (ϵ).[11]

The "physics" of the absorption process in solution has been extensively investigated and the results of several studies convincingly show that the nonequilibrium limit represents most suitable framework.[9,11] Effective strategies have also been devised to compute the solvation contribution to vertical excitation energies both for state specific[24] (SS) and linear response (LR) quantum mechanical methods.[25,26] In the former approaches, configuration interaction (CI) and complete active space self consistent field (CASSCF), a fully variational formulation of solvent effect on the excited state properties is achieved, by solving a different effective. Shrödinger equation for each state of interest.[24] In the latter models, random phase approximation [(RPA), TD-DFT calculations] excitation energies are computed directly, without using the exact excited state electron density.[25,26] Several papers have shown that SS and LR approaches are intrinsically different, and that the SS route should, in principle, lead to a more reliable and accurate determination of the solvation free energy variation associated with the change in the electron density upon excitation.[27–29] On these grounds, in a recent contribution we have proposed an effective SS implementation of the PCM/TD-DFT method,[29] which exploits the very recent availability of TD-DFT electron densities for excited electronic states as a by-product of the implementation of PCM/TD-DFT analytical derivatives.[30] On the balance, the treatment of the absorption process in solution can be thus considered well assessed.

The study of emission processes involves additional difficulties. On the one hand, solute and solvent relaxation cannot be totally decoupled. On the other hand, especially when dealing with ultrafast excited state decay and with broad fluorescence spectra, the main part of the observed fluorescence spectrum could come from the Franck-Condon region and the excited state population could be quenched before it reaches the excited state minimum. As discussed in detail in the next section, such a complex scenario can be tackled by studying some limiting cases, such as, for example, when it can be assumed that solute geometry relaxation is much faster than relaxation of the slow solvent degrees of freedom. On the contrary, for long living emitting species most of the contribution to the spectra comes from the excited state minimum (this is the case, for instance, for phosphorescence). In this latter case, for what concerns solvent contribution, the emission process can be seen as the inverse of the absorption processes, since slow solvent degrees of freedom remain equilibrated with the excited state density, whereas only fast degrees of freedom can be equilibrated with the ground state electron density. It is thus clear that a theoretical method aimed to the study of emission processes in solution should allow for a correct treatment of nonequilibrium solvent effects both on excited and ground states.

SS methods are intrinsically designed for allowing this possibility, even if the number of studies employing SS-PCM calculations for emission is still limited. On the other hand, since in standard LR-PCM calculations the excitation/emission energies are computed as poles of the frequency dependent linear response functions of the molecular system in the *ground state*, solvent is always fully equilibrated with the ground state electron density. Overcoming this limitation would be extremely important, since LR methods such as TD-DFT are among the most promising tools for studying the excited states of large size systems of biological and technological interest.[31] A first attempt has been made in a recent paper, where a first order corrected LR method has been presented,[20] but a self-consistent state specific LR/PCM method for the study of emission processes is not yet available.

Complementing our paper on the absorption process, we will try to fill this gap by presenting a state specific iterative version of the PCM/TD-DFT method, designed for the study of fluorescence and phosphorescence spectroscopies in solution. Next, the results of LR and SS PCM/TD-DFT methods are compared for the emission processes in solution of several representative compounds, namely, formaldehyde and three coumarin derivatives.

We will pay special attention to the treatment of equilibrium/nonequilibrium solvation effects on the emission process and to the influence of the dynamical solvation approach on excited state geometry optimizations in solution. Due to the enormous potential impact of LR-PCM excited state geometry optimizations on the study of excited states in solution,[31,32] it is indeed important to gain further insights about their reliability in different systems.

II. THEORETICAL BACKGROUND

In the PCM the solvent is described as a homogeneous dielectric, which is polarized by the solute. The latter is placed within a cavity in the solvent medium (built as the envelope of spheres centered on the solute atoms) and the proper electrostatic problem at the cavity surface is solved using a boundary element approach.[11]

The resulting reaction field contribution to the solute free energy (G) can be expressed as

$$G = \tfrac{1}{2}\mathbf{V}^{\dagger}\mathbf{q}, \tag{1}$$

where vector $\mathbf{V}$ collects the values of the solute's electrostatic potential and $\mathbf{q}$ are the apparent surface charges placed at the center of the surface *tesserae* (i.e., the small tiles which the cavity surface is finely subdivided in), where $\mathbf{V}$ is also computed.

In the latest version of the method[11] the polarization charges depend on the solute's electrostatic potential and, thus, on its density, through a general relationship of the form

$$\mathbf{q} = -\mathbf{D}\mathbf{V}, \tag{2}$$

where the square matrix $\mathbf{D}$ is related to cavity geometrical parameters and to the solvent dielectric constant ϵ.

Let us consider a generic excited electronic state (2), together with the corresponding ground state (1). As already discussed in Ref. 29, in SS methods the excited state equilibrium $[\mathcal{G}_{eq}(2)]$ free energy in solution thus explicitly depends on the excited state (2) density.

$$\mathcal{G}_{\mathrm{eq}}^{(2)} = \frac{1}{2}\sum_i q_i^{(2)} V_{i,\rho}^{(2)} = \frac{1}{2}\sum_i q_{i,f}^{(2)} V_{i,\rho}^{(2)} + \frac{1}{2}\sum_i q_{i,s}^{(2)} V_{i,\rho}^{(2)}. \tag{3}$$

The nonequilibrium $(\mathcal{G}_{\mathrm{eq}}^{(2)})$ free energy in solution involves also an explicit dependence on the density of the ground state (1),

$$\mathcal{G}_{\mathrm{neq}}^{(2)} = \frac{1}{2}\sum_i q_{i,f}^{(2)} V_{i,\rho}^{(2)} + \left(\sum_i q_{i,s}^{(1)} V_{i,\rho}^{(2)} - \frac{1}{2}\sum_i q_{i,s}^{(1)} V_{i,\rho}^{(1)}\right) + \left(\frac{1}{2}\sum_i q_{i,s}^{(1)} V_{i,f}^{(2)} - \frac{1}{2}\sum_i q_{i,s}^{(1)} V_{i,f}^{(1)}\right). \tag{4}$$

In the above equations q_f/q_s and V_f/V_s are the polarization charges and the corresponding potentials relative to the "fast" and "slow" solvent degrees of freedom. $V_{\rho}^{(n)}$ is instead the potential generated by the density of the state (n).

As anticipated in the introduction, the absorption process is ruled by nonequilibrium solvation, and thus the solvent contribution to the vertical excitation energy can be computed by using the following relationship:

$$\Delta G_{\mathrm{abs}} = \mathcal{G}_{\mathrm{neq}}^{(2)} - \mathcal{G}_{\mathrm{eq}}^{(1)}. \tag{5}$$

Soon after the electronic transition has occurred, the system starts evolving on the excited state potential energy surface (PES) toward its energy minimum. At the same time, slow solvent degrees of freedom start equilibrating on the excited state electron density. These two processes cannot be rigorously decoupled, especially when they exhibit similar time scales and we cannot thus expect that a single strategy is suitable to all the possible emission processes. In many cases, however, this complex scenario can be simplified by means of qualitative considerations on the properties of the solvent and/or of the excited potential energy surface. The equilibration of intramolecular degrees of freedom is faster than solvent equilibration except for very flat PES or when many low frequency motions are involved (large amplitude torsional motions, inversions, etc.). This is especially true in polar solvents and for electronic transitions involving significant variations of the excited state electron density. In such cases, indeed, time-resolved experiments suggest that the equilibration of the slow solvent degrees of freedom occurs on the picosecond time scale. This time should be long enough to assume that the excited electronic state has reach its minimum.

In the following we thus assume that the emission occurs from the excited state minimum, and we will focus our attention only on the solvent degrees of freedom.

A simple limiting case is that of ultrafast excited state decay, when only fast solvent degrees of freedom are expected to be in equilibrium with the excited state density. In this limit, ΔG_{em} can be computed exactly in the same way as ΔG_{abs},[29]

$$\Delta G_{\mathrm{em}} = \mathcal{G}_{\mathrm{neq}}^{(2)} - \mathcal{G}_{\mathrm{eq}}^{(1)}. \tag{6}$$

Of course, in this case excited state geometry optimizations should be also performed in the nonequilibrium limit.

Another simple limit is that of "very long" excited state lifetimes, which characterize, for instance, strongly fluorescent species. In this case, we can assume that all the solvent degrees of freedom are in equilibrium with the excited state density. The ground state $[\mathcal{G}_{\mathrm{eq}}^{(1)}]$ nonequilibrium free energy in solution describing the emission process can thus be obtained from Eq. (4), interchanging labels 1 and 2. The fast solvent degrees of freedom are equilibrated with the ground state electron density, whereas the slow ones are kept frozen to the value obtained in the equilibrium calculation of the excited state.

In this limit, excited state geometry optimizations should be performed with the solvent equilibrium limit and the solvent contribution to the fluorescence energy (ΔG_{em}) is

$$\Delta G_{\mathrm{em}} = \mathcal{G}_{\mathrm{eq}}^{(2)} - \mathcal{G}_{\mathrm{neq}}^{(1)}. \tag{7}$$

The above relationship is the most suitable also for treating phosphorescence, where states (2) and (1) correspond to T_0 and S_0, respectively.

The computation of the quantities involved in Eq. (6) and (7) is straightforward by using a generalization of the SS-PCM/TD-DFT method presented in Ref. 29, where the nonlinear problem of determining the polarization charges corresponding to excited state density is solved by using a self-consistent iterative procedure. Starting from a TD-DFT calculation *in vacuo* a first approximation to the state specific reaction field is computed using the electron density of the state of interest, by solving Eq. (2). In the next step, a TD-DFT calculation is performed in the presence of this first set of polarization charges, providing an updated excited state density and, consequently, a new set of polarization charges. This iterative procedure is continued until convergence on the reaction field is achieved. In the cases examined until now, 4/5 iterations are usually sufficient to reach a convergence $\leqslant 0.0001$ a.u. on the final energy. The final equilibrium and nonequilibrium energies of the state of interest are easily determined by adding the corrections obtained by Eq. (3) and (4) to the excited state energy provided by the TD calculation. Please note that, since in the latest implementation of the PCM method the wave function is directly computed in solution (without any preceding gas phase calculation), the

energy spent for the polarization of the solute with respect to the gas phase is automatically included in the computed free energy.

The treatment of nonequilibrium solvent effect is less straightforward when using standard LR-PCM/TD-DFT calculations. In this respect it is useful to briefly remind that the PCM contribution to the time dependent Kohn-Sham equations depends[25] on the term $\delta\phi(\mathbf{s}',\omega)$,

$$\delta\phi(\mathbf{s}',\omega)=\int_{\mathbf{R}^3}\frac{\delta\rho^{\mathrm{el}}(\mathbf{r}',\omega)}{|\mathbf{s}'-\mathbf{r}'|}d\mathbf{r}', \tag{8}$$

that formally corresponds to an electrostatic potential computed using the electron density variation ($\delta\rho^{\mathrm{el}}$) associated to the electronic transition in place of a specific electron density (ρ^{el}). The contribution from the PCM operator is then defined as

$$v^{\mathrm{PCM}}[\delta\rho^{\mathrm{el}}](\mathbf{r})=\int_\Gamma\int_\Gamma\delta\phi(\mathbf{s}',\omega)\mathcal{Q}(\epsilon_{\mathrm{opt}};\mathbf{s}',\mathbf{s})\frac{1}{|\mathbf{s}-\mathbf{r}|}d\mathbf{s}d\mathbf{s}', \tag{9}$$

if only the fast solvation degrees of freedom are equilibrated with the excited state density of the solute, and

$$v^{\mathrm{PCM}}[\delta\rho^{\mathrm{el}}](\mathbf{r})=\int_\Gamma\int_\Gamma\delta\phi(\mathbf{s}',\omega)\mathcal{Q}(\epsilon;\mathbf{s}',\mathbf{s})\frac{1}{|\mathbf{s}-\mathbf{r}|}d\mathbf{s}d\mathbf{s}', \tag{10}$$

when treating equilibrium solvation. In the nonequilibrium case, the PCM response matrix $\mathcal{Q}$ depends on the dielectric constant at optical frequency (ϵ_{opt}), whereas in the equilibrium case it depends on ϵ.

As anticipated in the introduction, besides the differences in treating nonequilibrium solvent effects on the excited state, in LR-PCM method the ground state is thus always fully equilibrated with the solvent degrees of freedom. As a consequence, in the nonequilibrium case the solvation contribution to the emission energy is computed as

$$\Delta G_{\mathrm{em}}(\mathrm{LR})=\mathcal{G}^{(2)}_{\mathrm{neq}}(\mathrm{LR})-\mathcal{G}^{(1)}_{\mathrm{eq}}, \tag{11}$$

whereas for long living excited state it is computed as

$$\Delta G_{\mathrm{em}}(\mathrm{LR})=\mathcal{G}^{(2)}_{\mathrm{eq}}(\mathrm{LR})-\mathcal{G}^{(1)}_{\mathrm{eq}}, \tag{12}$$

i.e., in standard LR-PCM the equilibrium solvation energy for the ground state is used in both cases.

III. COMPUTATIONAL DETAILS

Whenever not explicitly stated, geometry optimizations for the ground and the excited states have been performed at the PBE0/6-31G(d) (Ref. 33) and TD-PBE0/6-31G(d) (Ref. 34) level, respectively. The optimized geometries can be found in the supplementary materials.[35] The effect of basis set extension on the vertical excitation energies (VEEs) has been estimated by test computations with more extended 6-31+G(d,p) basis set.

Bulk solvent effects on the ground and the excited states have been taken into account by means of the latest developments[36] of PCM.[11] In equilibrium condition standard static dielectric constants at 298 K have been used, namely, 78.39 (water) and 24.55 (ethanol). The optical dielectric constants used in the nonequilibrium calculations are instead 1.776 (water) and 1.847 (ethanol), respectively. The united atom topological model[37] has been used for building the molecular cavity, defining the cavity radii according to the UA0 model.

All the calculations have been performed by using a development version of the GAUSSIAN package.[38]

IV. RESULTS

A. Formaldehyde

As a first step of our analysis we have computed the VEEs and the 0-0 transition energies (00TE) of the two lowest energy excited states of formaldehyde in aqueous solution, comparing the results obtained by the new SS approach [by using Eqs. (6) and (7)] with those provided by LR-PCM calculations [by using Eqs. (11) and (12)] both in the equilibrium and nonequilibrium limits. Please note that the difference between the equilibrium and non equilibrium results for 00TE provides an estimate of the importance of dynamic solvent effects for the excited state energy, since the solvation energy of the ground state in its minimum is always computed at the equilibrium level.

The excited state geometry has been optimized at the LR-PCM/PBE0/6-31G(d) level, in the solvent equilibrium limit. We have checked by test calculations that our results are not qualitatively changed if geometries optimized in the nonequilibrium limit are employed. For example, for the two formaldehyde excited states the SS-PCM results changes by less than 200 cm^{-1}, depending on the choice of the time regime to be used in the geometry optimizations. Only bulk solvent effects will be included in the calculations, even if hydrogen bond interactions with first solvation shell molecules should be explicitly taken into account in order to accurately study the excited state behavior of aldehydes in aqueous solution.[24] Quantitative reproduction of the experimental emission spectra of H_2CO in water is indeed outside the scope of the present paper.

As previously shown, the $S_0\rightarrow S_1$ transition in formaldehyde is a dipole forbidden $n\rightarrow\pi^*$ transition mainly corresponding to a highest occupied molecular orbital to lowest unoccupied molecular orbital (HOMO$\rightarrow$LUMO) excitation. Since geometry optimizations leads to a nonplanar minimum, this transition acquires some oscillator strength.

Inspection of Table I shows that equilibrium and nonequilibrium LR-PCM calculations provide very similar estimates of the VEE and of the 00TE, the difference between the two approaches being $\approx$100 cm^{-1}, in analogy with the findings of our previous study on absorption spectra.[29]

The difference between LR-PCM equilibrium and LR-PCM nonequilibrium calculations is instead significantly larger for the more intense $\pi\rightarrow\pi^*$ transition ($\approx$450 cm^{-1}).

The prediction of SS-PCM calculations are significantly different. Indeed for the S_1 transition, the difference between equilibrium and nonequilibrium results is $>$1000 cm^{-1},

TABLE I. Vertical emission energy and 0-0 transition energy (in cm^{-1}) of the two lowest energy $n\rightarrow\pi^*$ and $\pi\rightarrow\pi^*$ transitions of formaldehyde calculated in aqueous solution, according to different solvation models, by PCM/TD-PBE0/6-31G(*d*) calculations on PCM/PBE0/6-31G(*d*) optimized geometries. Oscillator strengths in parentheses and excited state dipole moments (in debyes) in italics. [Emission energy computed in the gas phase: 24100 cm^{-1} ($n\rightarrow\pi^*$) and 44500 cm^{-1} ($\pi\rightarrow\pi^*$).]

	Emission energy		0-0 transition energy	
	Nonequilibrium solvation	Equilibrium solvation	Nonequilibrium solvation	Equilibrium solvation
		$n\rightarrow\pi^*$		
SS	25400(0.00)*2.1*[a]	24050(0.00)*2.0*	31560(0.00)[b]	30540(0.00)
LL	24830(0.00)*2.1*	24700(0.00)*2.0*	30990(0.00)	30860(0.00)
		$\pi\rightarrow\pi^*$		
SS	44410(0.015)*2.8*[c]	43600(0.015)*2.7*	64100(0.015)	63480(0.015)
LR	43660(0.020)*2.8*	43230(0.030)*2.7*	63340(0.020)	62910(0.030)

[a]Ground state dipole moment: 3.0.
[b]Ground state dipole moment: 2.8.
[c]Ground state dipole moment: 3.5 (computed at the geometry of the ground state minimum).

while the values for the S_2 transition are smaller ($\approx$700 cm^{-1}), though still larger than the estimate provided by LR-PCM calculations.

As a further check of the reliability of the SS-PCM approach we have computed the solvation energy of H_2CO at the equilibrium structure of its triplet state, that can indeed be obtained by using "standard" PCM-PBE0, in the accurate implementation used for ground state calculations.

PCM/PBE0 6-31G(*d*) calculations predict that in aqueous solution the triplet minimum is stabilized by 770 cm^{-1} with respect to the gas phase. We can compute the same quantity starting from the singlet ground state by using TD-PBE0 calculations, looking for the lowest energy $S_0\rightarrow T_1$ transition both in the gas phase and in solution. The T_1 electron density provided by the TD-PBE0 calculations is similar to that obtained by PCM/PBE0 ground state calculations. As a matter of fact, Mulliken population analysis performed on the T_1 excited density indicates that the atomic Mulliken population on the oxygen atom is −0.20 a.u., that on Carbon Atom −0.29 a.u., and that on the Hydrogen Atoms 0.245 a.u. according TD-PBE0 calculations. Those values are very close to those provided by PBE0 calculations: −0.22 a.u. (oxygen atom), −0.24 a.u. (carbon atom), and 0.23 a.u. (hydrogen atoms). As a consequence, the solvation energy computed for the triplet at the PCM/TD-PBE0 level is expected to be very similar to that obtained at the PCM/PBE0 level.

Actually, LR-PCM/TD-PBE0/6-31G(*d*) calculations provide a much lower estimate, $\approx$60 cm^{-1}. This value is the same when computed both at the equilibrium and at the nonequilibrium level, as it could be expected due to the vanishing oscillator strength of the $S_0\rightarrow T_1$ transition (*vide supra*). SS-PCM/TD-PBE0/6-31G(*d*) calculations (at the equilibrium level) predict instead a solvation energy of $\approx$870 cm^{-1}, in good agreement with the value obtained by ground state PCM/PBE0 calculations.

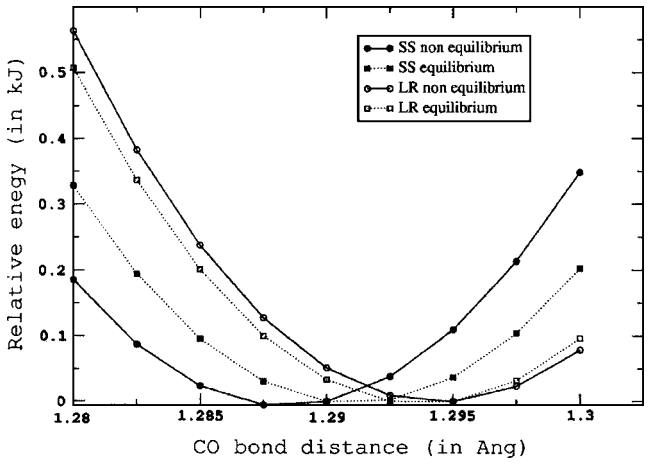

FIG. 1. Relative energy (in kilojoules) of the lowest energy $n\rightarrow\pi^*$ transition as a function of the CO bond length in formaldehyde. The energy of each curve has been scaled with respect to its minimum.

B. Geometry optimizations

SS-PCM excited state analytical gradients are not available, and, in any case, the iterative implementation of SS-PCM would probably make SS-PCM geometry optimizations rather cumbersome. On the other hand LR-PCM TD-DFT excited state geometry optimizations generally provide reliable excited state geometries and frequencies in the condensed phase.[9,12] It is thus important to verify if the use of SS-PCM can lead to significantly different excited state geometries. To this end we have computed the energy of the lowest energy excited state of formaldehyde for different CO bond lengths, by using both SS-PCM/TD-PBE0/6-31G(*d*) and LR-PCM/TD-PBE0/6-31G(*d*) single point calculations (see Figs. 1 and 2). The remaining geometrical parameters are kept frozen to their value in the excited state minima, obtained by LR-PCM/TD-PBE0/6-31G(*d*) geometry optimizations.

Figures 1 and 2 show that the four approaches considered provide similar estimates of the CO equilibrium bond length. As a matter of fact, LR-PCM/TD-PBE0/6-31G(*d*) calculations predict the S_1 state has an energy minimum for a

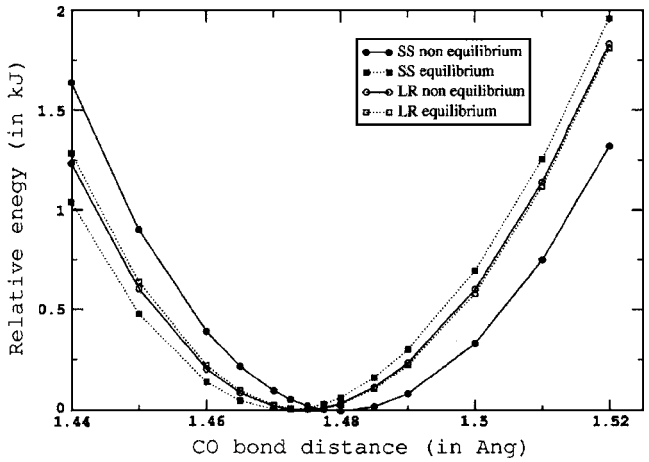

FIG. 2. Relative energy (in kilojoules) of the lowest energy $\pi\rightarrow\pi^*$ transition as a function of the CO bond length in formaldehyde. The energy of each curve has been scaled with respect to its minimum.

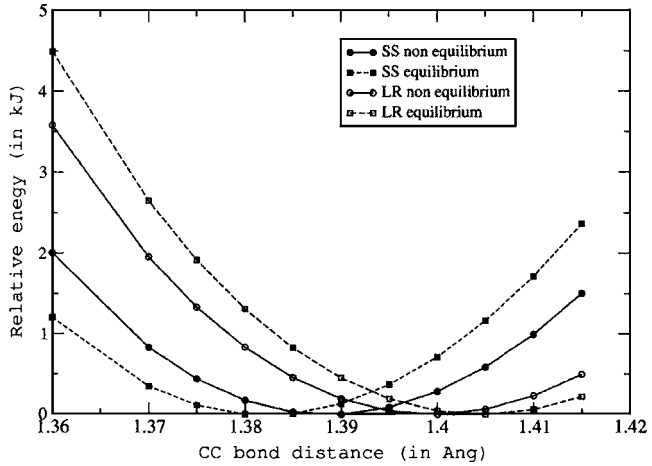

FIG. 3. Relative energy (in kilojoules) of the lowest energy $S_0 \rightarrow S_3$ transition as a function of the CC bond length in nitroethene. The energy of each curve has been scaled with respect to its minimum.

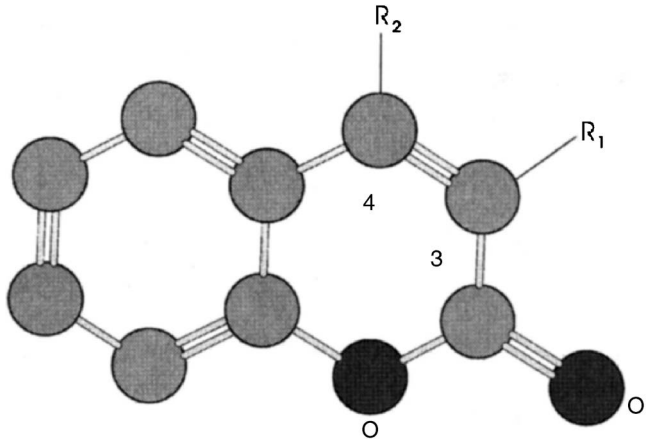

FIG. 4. Schematic drawing of the three coumarin derivatives examined in the present study R_1, R_2=H: Coumarin; R_1=CH_3, R_2=H: 3-methylcoumarin; and R_1=H, R_2=CH_3: 4-methylcoumarin.

CO bond length of 1.295 Å according to both equilibrium and nonequilibrium approaches. The values provided by SS-PCM calculations are extremely similar, being 1.288 and 1.290 Å, at the nonequilibrium and equilibrium levels, respectively.

This picture is confirmed also by the analysis of the results concerning the S_2 state. LR-PCM calculations provide for the equilibrium CO bond distance a value (1.475 Å) intermediate between those predicted by SS-PCM calculations, i.e., 1.473 Å (at the equilibrium level) and 1.478 Å (at the non equilibrium level).

It is noteworthy that while TD-PBE0/6-31G(*d*) geometry optimizations in the gas phase predict for the energy minimum of the S_1 state a CO bond distance (1.295 Å) similar to that obtained in aqueous solution, the discrepancy between the results of gas phase and solvent geometry optimizations is much larger for the S_2 state. The equilibrium CO bond distance computed in the gas phase is indeed 1.445 Å, significantly shorter than that of the results obtained both at the SS-PCM and LR-PCM levels.

Finally, both for S_1 and S_2 the PESs computed by the different solvent approaches exhibit very similar curvature, suggesting that the different computational approaches would provide similar values for the CO stretching frequency. If the four energy curves are fitted by a quadratic expression, the computed values for the force constants are indeed extremely close, within 1.5% and 5% for the S_1 and the S_2 states, respectively.

Both the excited states considered for formaldehyde have quite small dipole moments, being less polar than the ground state. In order to verify how excited state geometry optimizations in solution behave for electronic transitions involving a significant variation in the total electronic dipole moment, we have studied the $S_0 \rightarrow S_3$ transition in nitroethene. This electronic transition, mainly corresponds to a HOMO→LUMO excitation, is quite intense (oscillator strength ≈0.2) and it is associated to a significant increase of the electric dipole moment (≈2 D). The energy of this transition has been studied as a function of the CC bond length (see Fig. 3), while the remaining geometrical parameters have been frozen at the values of the excited state minimum (according to LR-PCM/TD-PBE0/6-31G(*d*) excited state geometry optimizations in aqueous solution).

It is clear that in this case, SS-PCM/TD-PBE0 and LR-PCM/TD-PBE0 methods provide different estimates of the C–C equilibrium bond distance. The former approach predicts indeed smaller values: 1.380 and 1.390 Å, at the equilibrium and nonequilibrium levels, respectively. The corresponding values provided by LR-PCM/TD-PBE0 calculations are 1.405 and 1.400 Å, respectively. It is worth of highlighting that the excited state dipole moment slightly increases when the C–C bond length decreases: equilibrium SS-PCM/TD-PBE0 calculations predict that for a C–C bond length=1.36 Å it is 7.10 D, whereas for a C–C bond length=1.4 Å it is 7.0 D. On the other hand, the intensity of the electronic transition increases with the C–C bond distance, from 0.20 to 0.22 in the range of C–C bond lengths examined.

C. Coumarin

As a further check for the reliability of the new methodology, we have computed the vertical emission energies of the $S_1 \rightarrow S_0$ transition for three coumarin derivatives (see Fig. 4 in ethanol solution), by using equilibrium LR-PCM and SS-PCM calculations. The three molecules examined belong to a large group of coumarins thoroughly investigated by means of LR-PCM/TD-PBE0 calculations in a recent study.[32] The authors of this study found a good agreement between the computed VEEs and the experimental maxima of the fluorescence band, although the computed values are, in general, blueshifted with respect to the experimental ones. Before commenting on our results it is important to remember that the position of the maximum of a fluorescence band does not necessarily coincide with the VEE, since it depends also on the vibrational characteristics of ground and excited electronic states through Franck-Condon factors. While effective procedures are being developed both for harmonic/anharmonic frequency computations[41,42] and for the evalua-

TABLE II. Vertical emission energy (in cm^{-1}) of the lowest energy electronic transition in three coumarin derivatives according to different solvation models, by PCM/TD-PBE0/6-31G(*d*) calculations on PCM/PBE0/6-31G(*d*) optimized geometries. Oscillator strengths in parentheses. The value including zero point vibrational corrections are given in italics. [Emission energy computed in the gas phase on the gas phase minima: 28 900 (coumarin), 29 500(3-methylcoumarin), and 27 100(4-methylcoumarin). Emission energy computed in the gas phase on the minima optimized in solution: 29 700 (coumarin), 30 100(3-methylcoumarin), and 29 400-methylcoumarin.]

	6-31G(*d*)		6-31+G(*d*,*p*)		
	SS-Eq	LR-Eq	SS-Eq	LR-Eq	
coumarin	27 600(0.07)*26 450*	29 000(0.24)*27 850*	28 100(0.09)	28 500(0.27)	25 600[a]
3-methylcoumarin	30 150(0.19)*29 050*	29 000(0.47)*27 900*	29 600(0.21)	28 350(0.53)	26 700[a]
4-methylcoumarin	29 150(0.09)*28 050*	29 300(0.28)*28 200*	28 800(0.10)	28 800(0.33)	26 100[b]

[a]Maximum of the fluorescence band in ethanol at 77 K (Ref. 39).
[b]Maximum of the fluorescence band in ethanol at room temperature (Ref. 40).

tion of FC factors,[9] these terms will not be considered here, because the focus of the present study is on electronic effects.

Bearing this caveat in mind, the findings of Ref. 32 are confirmed by the results reported in Table II. The LR-PCM results are indeed blueshifted with respect to the experimental ones, even when zero point vibrational correction are included. 3-methylcoumarin is the compound with the smallest discrepancy with respect to experiments. Actually, LR-PCM calculations predict that 3-methylcoumarin exhibits the lowest energy vertical emission among the compounds examined, whereas the opposite result is found experimentally. Not surprisingly (*vide infra*) 3-methylcoumarin is also the molecule with the largest oscillator strength.

The SS-PCM/TD-DFT results are more consistent with the experimental ones. Indeed the discrepancy with experiments is smaller than that found at the LR-PCM/TD-DFT level. When nonequilibrium solvent effects on the ground state are considered the emission energy decreases: the ground state is indeed destabilized, since the slow solvation charges are those optimized for the excited state. Furthermore, it is remarkable that not only the relative position of the emission band in the three compounds examined is correctly reproduced, but also the differences among the three VEEs [especially when the more extended 6-31+G(*d*,*p*) basis set is used] match almost quantitatively the differences between the experimental band maxima.

V. DISCUSSION AND CONCLUDING REMARKS

In this study we have presented the first state specific implementation of PCM/TD-DFT calculations, allowing for a rigorous treatment of dynamical solvent effects on fluorescence and phosphorescence spectra. By exploiting the availability of the excited state electron density and using an iterative procedure it is possible to include nonequilibrium solvent effects on the emission process energy, thus being able to treat emission and absorption processes on the same footings.

Comparison between SS and LR results for several test cases allows gaining further insights about the intrinsic differences between the two approaches. When applied to the study of the emission from the dark S_1 state in formaldehyde, LR-PCM/TD-PBE0 calculations predict a vanishingly small difference between the equilibrium and nonequilibrium results. Analogously the predicted solvation energy of the T_1 state is close to zero. This result can be explained on the ground of the analysis performed in our previous paper,[29] where it is shown that in the LR-PCM approach the difference between equilibrium and nonequilibrium solvation energies is proportional to the transition density matrix between the two states (μ_{01}^{tr}), thus vanishing for forbidden transitions. On this ground it is also possible to explain why geometry optimization of nitroethene favors slightly longer C–C bond distances and also why the lowest emission energy among the coumarin derivatives examined is obtained for the transition exhibiting the largest oscillator strength.

On the other hand, SS-PCM/TD-PBE0 calculations allow a more balanced description of equilibrium and nonequilibrium solvation energies, and when applied to the study of the phosphorescence in formaldehyde they provide very similar results to those obtained by using a standard "ground state" PCM-DFT approach. The difference between equilibrium and nonequilibrium results is larger for the $n \rightarrow \pi^*$ transition than for the $\pi \rightarrow \pi^*$ one, i.e., the opposite of what predicted at the LR-PCM level. Also this result is consistent with the previous analysis of the SS-PCM method applied to absorption spectra. In SS methods, indeed, equilibrium and nonequilibrium solvation are proportional to the excited state dipole moment and their difference is due to the sum of two contributions, depending on the difference and on the square of the difference between the excited and the ground state dipole moments, respectively. It is thus not surprising that for the S_3 state of nitroethene the equilibrium C–C bond length is shorter (with respect to LR-PCM results), leading to a slightly larger dipole moment.

When applied to the study of the emission process of three coumarin derivatives SS-PCM/TD-PBE0 calculations provide accurate results, with a discrepancy with respect the experimental band maxima lower than $\approx$0.2 eV, and reproduce substituent effects on the position of the fluorescence band maximum. Since our previous study shows a remarkable accuracy also in the analysis of the absorption process, it is now possible to characterize in a coherent way all the steps involved in the process of electron excitation and emission. Furthermore, the SS-PCM/TD-DFT method is not much more computationally expensive than LR-PCM/TD-

DFT, and thus it can be applied without significant problems to fairly large molecules, providing a very useful tool for studying many excited state processes in the condensed phase, for systems of biological and technological interest. There is obviously the drawback that SS-PCM/TD-DFT geometry optimizations are not yet possible and, due to the intrinsic iterative nature of this method, would be rather cumbersome.

An effective strategy would thus be complementing the results of LR-PCM/TD-DFT geometry optimizations, that have already shown a good accuracy, by single point SS-PCM calculations. Actually, the results of the present study confirm the general reliability of "standard" LR-PCM method that is able to provide qualitatively correct estimates of vertical excitation energies. In most of the systems we have examined the maximum discrepancy between SS-PCM and LR-PCM emission energies is $<1000\ \mathrm{cm}^{-1}$. Furthermore, in many systems a good agreement between LR-PCM/TD-DFT results and experimental absorption and emission spectra has been found.[11,31] It has indeed been shown[27] that at the zeroth order, related to the interaction with the slow solvation degrees of freedom, LR and SS approaches are identical. Confirming the results of our previous paper,[29] LR-PCM results can be less reliable when dealing with electronic transitions involving a large variation of the electron density in polar solvents. Indeed the largest discrepancy between LR-PCM and SS-PCM results ($\simeq 1400\ \mathrm{cm}^{-1}$) is found for coumarin.

The same considerations hold also for the reliability of LR-PCM geometry optimizations. Our preliminary analysis provides positive indications, since no significant discrepancies are predicted with respect to SS-PCM calculations. As a consequence, in most of the cases, the LR-PCM geometry optimizations are expected to provide a better approximation to the "real" excited state in solution than TD-DFT gas phase calculations. On this respect, it is worth of noting that when computing the emission energies of coumarin-methylcoumarin 4-methylcoumarin in the gas phase the agreement with the experimental results is better when the excited state minima computed at the LR-PCM level are used (see footnotes of Table II). Furthermore, there is a growing number of indications that the absorption spectra computed by using the excited state geometries and frequencies provided by LR-PCM TD-DFT geometry optimizations are in good agreement with the experimental ones.[9,12]

The only electronic processes for which LR-PCM/TD-DFT geometry optimizations should be considered with some caution are, again, those characterized by large electron density variation and by a very small oscillator strength, or when a very accurate description of the excited state geometry is sought (especially in the study of electronic transition involving changes in floppy vibrational degrees of freedom).

When dealing with this kind of transitions, especially within polar solvents, a parallel SS-PCM/TD-DFT analysis is highly desirable, as well as when looking for an accurate description of time dependent solvent relaxation effect. In these cases, a preliminary check could be computing the SS-PCM energy of the excited state minima computed both at the LR-PCM/TD-DFT level (in the equilibrium or nonequilibrium limit) and *in vacuo*. However, it is important to highlight that calculation of fluorescence energies at the SS-PCM TD-DFT level does not necessarily rely on LR-PCM geometry optimizations, but it can complement any method able to provide accurate excited state minima in solution.

Together with the previous studies in this field, the present research confirms the high degree of accuracy and the flexibility of the PCM method for the study of ground and excited states in a large number of chemical processes. It is, obviously, always important to bear in mind that solvation dynamics is a very complex phenomenon, and that many aspects cannot be captured by pure continuum models, but require the inclusion of some explicit solvent molecules. In these latter cases, however, the inclusion of bulk solvent effects by means of continuum models can significantly decrease the number of solvent molecules to be explicitly considered in the calculations.

ACKNOWLEDGMENTS

All the calculations have been performed using the advanced computing facilities of the VILLAGE node at the University Federico II, Naples (village.unina.it). Also, two of the authors (R.I. and V.B.) acknowledge Dr. Fabrizio Santoro for useful discussions and Gaussian Inc., MUIR, and INSTM for financial support.

[1] B. Valeur, *Molecular Fluorescence* (Wiley-VCH, Berlin, 2001); J. R. Albani, *Structure and Dynamics of Macromolecules: Absorption and Fluorescence Studies* (Elsevier, New York, 2004).
[2] B. L. Van Duuren, Chem. Rev. (Washington, D.C.) **63**, 325 (1963); X. Michalet, S. Weiss, and M. Jager, *ibid.* **106**, 1785 (2006).
[3] T. Gustavsson, A. Banyasz, E. Lazzarotto, D. Markovitsi, G. Scalmani, M. J. Frisch, V. Barone, and R. Improta, J. Phys. Chem. B **128**, 607 (2006); T. Gustavsson, N. Sarkar, E. Lazzarotto, D. Markovitsi, V. Barone, and R. Improta, J. Phys. Chem. B **110**, 12843 (2006); D. Markovitsi, F. Talbot, T. Gustavsson, D. Onidas, E. Lazzarotto, and S. Marguet, Nature (London) **441**, E7 (2006).
[4] M. Olivucci and A. Sinicropi, in *Computational Photochemistry*, edited by M. Dlivucci (Elsevier, Amsterdam, 2005), Vol. 16; A. Dreuw and M. Head-Gordon, Chem. Rev. (Washington, D.C.) **105**, 4009 (2005); K. Andersson and B. O. Roos, *Modern Electronic Structure Theory*, edited by D. R. Yarkony (World Scientific, New York, 1995), Vol. 1, p. 55.
[5] R. Bergen, O. Fischer, and M. Klessinger, J. Phys. Chem. A **102**, 7157 (1998); S. Grimme, Rev. Comput. Chem. **20**, 153 (2004); V. Rodriguez-Garcia, K. Yagi, K. Hirao, S. Iwata, and S. Hirata, J. Chem. Phys. **125**, 014109 (2006); K. Burke, J. Werschnik, and E. K. U. Gross, *ibid.* **123**, 62206 (2005).
[6] M. Dierksen and S. Grimme, J. Chem. Phys. **120**, 3544 (2004).
[7] M. Dierksen and S. Grimme, J. Phys. Chem. A **108**, 10225 (2004).
[8] M. Dierksen and S. Grimme, J. Chem. Phys. **122**, 244101 (2005).
[9] F. Santoro, R. Improta, A. Lami, J. Bloino, and V. Barone, J. Chem. Phys. **126**, 084509 (2007); **126**, 169903(E) (2007).
[10] F. Santoro, A. Lami, R. Improta, and V. Barone, J. Chem. Phys. **126**, 184102 (2007).
[11] J. Tomasi, B. Mennucci, and R. Cammi, Chem. Rev. (Washington, D.C.) **105**, 2999 (2005).
[12] R. Improta, V. Barone, and F. Santoro, Angew. Chem., Int. Ed. **46**, 405 (2007).
[13] U. F. Rohrig, I. Frank, J. Hutter, A. Laio, J. Vande Vondele, and U. Rothlisberger, ChemPhysChem **4**, 1177 (2003); H. C. Georg, K. Coutinho, and S. Canuto, J. Chem. Phys. **126**, 034507 (2007); O. Crescenzi, M. Pavone, F. De Angelis, and V. Barone, J. Phys. Chem. B **109**, 445 (2005); K. Aidas, J. Kongsted, A. Osted, K. V. Mikkelsen, and O. Christiansen, J. Phys. Chem. A **109**, 8001 (2005); G. Brancato, N. Rega, and V. Barone, J. Chem. Phys. **125**, 164515 (2006); M. Pavone, P. Cimino, F. De Angelis, V. Barone, J. Am. Chem. Soc. **128**, 4338 (2006).
[14] J. Tomasi and M. Persico, Chem. Rev. (Washington, D.C.) **94**, 2027

(1994).
[15] C. J. Cramer and D. G. Truhlar, Chem. Rev. (Washington, D.C.) **99**, 2161 (1999).
[16] M. V. Basilevskyi, D. F. Parsons, and M. V. Vener, J. Chem. Phys. **108**, 1103 (1998).
[17] M. D. Newton and H. L. Friedman, J. Chem. Phys. **88**, 4460 (1988).
[18] P. G. Wolynes, J. Chem. Phys. **86**, 5133 (1987).
[19] I. V. Rostov, M. V. Basilevsky, and M. D. Newton, in *Simulation and Theory of Electrostatic Interactions in Solution*, edited by L. R. Pratt and G. Hummer (American Institute of Physics, New York, 1999).
[20] M. Caricato, B. Mennucci, J. Tomasi, F. Ingrosso, R. Cammi, S. Corni, and G. Scalmani, J. Chem. Phys. **124**, 124520 (2006).
[21] M. Caricato, F. Ingrosso, B. Mennucci, and J. Tomasi, J. Chem. Phys. **122**, 154501 (2005).
[22] M. Cossi and V. Barone, J. Phys. Chem. A **104**, 10614 (2000).
[23] M. A. Aguilar, J. Phys. Chem. A **105**, 10393 (2001).
[24] M. Cossi and V. Barone, J. Chem. Phys. **112**, 2427 (2000); M. Cossi, V. Barone, and M. A. Robb, *ibid.* **111**, 5295 (1999).
[25] M. Cossi and V. Barone, J. Chem. Phys. **115**, 4708 (2001).
[26] R. Cammi, B. Mennucci, and J. Tomasi, J. Phys. Chem. A **104**, 5631 (2000).
[27] R. Cammi, S. Corni, B. Mennucci, and J. Tomasi, J. Chem. Phys. **122**, 104513 (2005).
[28] S. Corni, R. Cammi, B. Mennucci, and J. Tomasi, J. Chem. Phys. **123**, 134512 (2005).
[29] R. Improta, V. Barone, G. Scalmani, and M. J. Frisch, J. Chem. Phys. **125**, 054103 (2006).
[30] G. Scalmani, M. J. Frisch, B. Mennucci, J. Tomasi, R. Cammi, and V. Barone, J. Chem. Phys. **124**, 094107 (2006).
[31] T. Gustavsson, A. Banyasz, E. Lazzarotto, D. Markovitsi, G. Scalmani, M. J. Frisch, V. Barone, and R. Improta, J. Am. Chem. Soc. **128**, 607 (2006); F. Santoro, V. Barone, T. Gustavsson, and R. Improta, *ibid.* **128**, 16312 (2006); R. Improta and V. Barone, *ibid.* **126**, 14320 (2004).
[32] D. Jacquemin, E. A. Perpéte, G. Scalmani, M. J. Frisch, X. Assfeld, I. Ciofini, and C. Adamo, J. Chem. Phys. **125**, 164324 (2006).
[33] C. Adamo and V. Barone, J. Chem. Phys. **110**, 6158 (1999); M. Enzerhof and G. E. Scuseria, *ibid.* **110**, 5029 (1999).
[34] C. Adamo, G. E. Scuseria, and V. Barone, J. Chem. Phys. **111**, 2889 (2000).
[35] See EPAPS Document No. E-JCPSA6-127-508729 for the coordinates of all the relevant energy minima. This document may be retrieved through a direct link in the online article's HTML reference section or via the EPAPS homepage (http://www.aip.org/pubservs/epaps.html).
[36] M. Cossi, G. Scalmani, N. Rega, and V. Barone, J. Chem. Phys. **117**, 43 (2002).
[37] V. Barone, M. Cossi, and J. Tomasi, J. Chem. Phys. **107**, 3210 (1997).
[38] M. J. Frisch, G. W. Trucks, H. B. Schlegel *et al.*, GAUSSIAN, development version, revision F.01, Gaussian, Inc., Wallingford, CT, 2006.
[39] W. W. Mantulin and P. S. Song, J. Am. Chem. Soc. **95**, 5122 (1973).
[40] C. E. Wheelcock, J. Am. Chem. Soc. **81**, 1348 (1959).
[41] V. Barone, J. Chem. Phys. **101**, 10666 (1994).
[42] V. Barone, J. Chem. Phys. **122**, 014108 (2005).